ON THE CORRELATION OF TROPOSPHERIC ZENITH PATH DELAY AND STATION CLOCK ESTIMATES IN GEODETIC GNSS FREQUENCY TRANSFER

U. Weinbach[(1),(2)], S. Schön[(1),(2)]

[(1)]Institut für Erdmessung (IfE)
Leibniz Universität Hannover
Schneiderberg 50, 30167 Hannover, Germany
Email: weinbach@ife.uni-hannover.de

[(2)]Centre for Quantum Engineering and Space Time Research
Leibniz Universität Hannover
Hannover, Germany

INTRODUCTION

Time and frequency transfer based on Global Navigation Satellite System (GNSS) code and carrier phase observations along with elaborate geodetic adjustment models have become a standard tool for high-precision clock comparisons. This development has been facilitated by the availability of highly precise satellite orbits and clock corrections through the International GNSS Service (IGS) [1] enabling un-differenced processing of data from a single receiver known as Precise Point Positioning (PPP). With the PPP approach few mm static positioning accuracy can be achieved for 24 h observation sessions [2]. In addition PPP allows for highly precise time and frequency comparisons between remote clocks. PPP based frequency transfer at the level of $\sigma_y=2\cdot10^{-15}$ at one day averaging time are now regularly reported [3], [4]. This is however significantly worse than we would expect considering the Allan deviation $\sigma_y \approx 5\cdot10^{-13}$ typically achieved at 30 s averaging time. Among the reasons for the degraded performance are errors induced by incorrect modeling of the tropospheric propagation delays. Without systematic modeling deficiencies and assuming proper temperature stabilization of the receivers, PPP could provide us with a frequency transfer precision of well below $1\cdot10^{-15}$ at one day averaging time [5].

Within the geodetic community the modeling of the tropospheric propagation delays has been recognized as one of the major error sources limiting the accuracy of the station height estimates in GNSS analysis. Since all visible satellites are clustered above the receiving station an error in the tropospheric propagation delay will predominately be mapped into station height and clock estimates. Due to these mathematical correlations and the need to estimate a receiver clock offset for every observation epoch, the clock estimates will generally absorb most of the short-term troposphere modeling errors. In contrast, the station height is only affected by the average troposphere error during the entire computing batch (typically 24 hours).

In this contribution we will give an overview of troposphere modeling in GNSS analysis and show approximate relations for the propagation of errors of the tropospheric zenith path delays into the station clock estimates. Furthermore, the usage of low elevation data is shown to reduce peak variations in both tropospheric delay and receiver clock estimates. Finally, we study the impact of using different mapping functions and hydrostatic zenith delay models on the estimated receiver clock offsets.

TROPOSPHERE MODELING

The electromagnetic signals broadcasted by the GNSS satellites are subject to significant delays in the neutral part of the earth's atmosphere, mainly the troposphere. Typical values are 2.4 m for an observation in zenith direction and up to 24 m at 5° elevation. Since the delay induced by the troposphere is the same for all GNSS signals in use, it cannot by estimated or

eliminated by using multiple frequencies as it is the case for the ionospheric delay. This makes the tropospheric propagation delay one of the most important error sources for high precision GNSS applications, which requires careful modeling.

In GNSS data analysis the tropospheric delay is usually modeled by a zenith delay parameter that is related to the slant delay associated to a certain observation by a so called mapping function. All mapping functions in use today assume azimuthal symmetry, i.e. they solely depend on the elevation angle of the satellite. The total tropospheric zenith delay (TZD) is usually expressed as the sum of a hydrostatic (ZHD) and a wet (ZWD) component, with corresponding mapping functions mf_h and mf_w. The complete expression for the tropospheric slant delay (T) for an observation at elevation angle e then reads [6]:

$$T(e) = mf_h(e) \cdot ZHD + mf_w(e) \cdot ZWD \tag{1}$$

The hydrostatic part of tropospheric zenith delay can be determined quite accurately using pressure values observed at the GNSS antenna site. It amounts to approximately 2.3 m at sea level and makes up approximately 90 % of the total tropospheric delay [6]. Various models have been established to derive the hydrostatic zenith delay from surface pressure or a standard atmosphere, with the one by Saastamoinen being the most popular and recommended in the latest IERS standards [7]. More recently ZHDs from ray-tracing through numerical weather models (NWM) have been made available [8], that allow the determination of accurate ZHD values even if no pressure observation are available.

In contrast to the hydrostatic part of the tropospheric delay, the wet component cannot be estimated from surface meteorological data at the level of accuracy required. Sophisticated and expensive monitoring devices like Water Vapor Radiometers (WVR) or Raman Lidars sensing the amount of preciptable water vapor in the troposphere have to be used to get an accurate value for the ZWD but the operation of such devices and the calibration is difficult [9]. Thus for most high precision applications such as Precise Point Positioning PPP the wet part of the zenith delay has to be estimated within the least-squares adjustment. The parameterization needs to take into account the time-varying nature of the zenith delay. For this investigation the ZWD was modeled as a piece-wise linear parameter with 15 minutes intervals.

CORRELATIONS AND ERROR PROPAGATION

The correlations between station height, troposphere and receiver clock estimates have been studied by different authors in the past with primary focus on the relationship of height and troposphere [e.g. 10]. Based on analytical considerations Dach et al [11] give a correlation coefficient between clock off set and troposphere zenith delay of -0.980 for an elevation cut-off angle of 15° and elevation dependent weighting at an equatorial site. According to this study the correlation coefficient can be reduced to -0.91 by lowering the cut-off angle to 5°. The correlation is reduced because the partial derivatives of the observation equation with respect to clock offset and tropospheric zenith delay are highly different at low elevations.
The correlation between troposphere zenith path delays and clock offsets is particularly harmful for frequency transfer because both parameter types have to be estimated with a high temporal resolution. Therefore short-term troposphere modeling errors will propagate to a large degree into the receiver clock estimates.

IIMPACT OF ZWD ERRORS ON PPP CLOCK ESTIMATES

In order to study the propagation of troposphere errors into the receiver clock offsets we have added a constant 1 cm bias to the estimated wet tropospheric zenith path delay. The receiver clock was then estimated in a back-substitution step with the coordinates and carrier phase ambiguities fixed to the values from the unbiased solution. The cut-off angle was set to 5° and elevation-dependent observation weighting ($\sin^2 e$) has been applied. After the introduction of the 1 cm bias, we observed a shift in the estimated receiver clock time series of -2.4 centimeters (Fig. 1). After increasing the elevation cut-off angle to 15° the shift was still -1.4 cm. These results are in good agreement with the findings by Hackman and Levine [12] who reported a factor of 1.5 for a cut-off angle of 15° based on clock and troposphere differences between two stations. The values in table 1 can also be used as a rule of thumb for estimating the influence of short-term errors in the ZWD on the receiver clock estimates. Note, however, that the values only apply if observations at low elevation are not obstructed. For our investigation we selected the IGS station WTZR which has almost no obstruction down to an elevation angle of 5°.

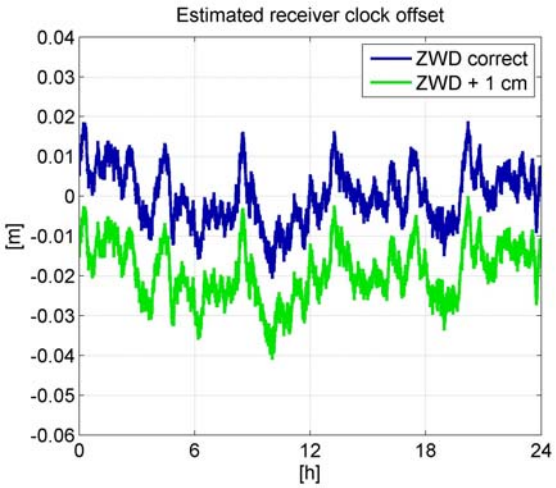

Fig. 1. PPP receiver clock offset at WTZR with and without a 1 cm troposphere bias (elevation cut-off 5°)

Tab. 1. Relationship between troposphere zenith path delay error and estimated clock offset

Cut-off angle	ΔZWD [m]	ΔCLK [ps]	ΔCLK·c [m]	Ratio
5	0.01	-78.7	-0.024	-2.4
10	0.01	-54.9	-0.017	-1.7
15	0.01	-45.5	-0.014	-1.4

IMPACT OF DIFFERENT ELEVATION CUT-OFF ANGLES

The delays induced by the troposphere quickly increase at low elevations, making the estimation of the ZWD more stable. On the other hand, low elevation observations suffer from an increased noise level, more frequent cycle slips and multi-path effects. Therefore, observations at low elevations have been down weighted with $\sin^2(e)$ reducing their impact on the solution. In order to study the influence of different elevation cut-off angles on the clock and troposphere estimates we compared a PPP solution with 15° elevation cut-off and a solution using observations down to 5° elevation. IGS final orbits and clocks have been used and the wet troposphere delay was modeled by a piece-wise linear ZWD with 15 minute resolution, mapped with the Global Mapping Function (GMF) [13]. Apart from a shift, we find that the peak variations of the estimated clock time series are reduced when observations at low elevations are included in the analysis (Fig. 2). The improvement can also be seen in the corresponding Allan deviations (Fig. 3). We therefore conclude, that using observation data down to an elevation angle of 5° in combination with a proper weighting scheme can improve the estimation of ZWDs and clock offsets. In practice, however, the impact of multipath, receiver tracking characteristics and other site-specific effects, also has to be taken into account.

In addition to the shift of the estimated receiver clock offsets the difference of the station height with respect to the weekly IGS solution changed by almost 1 cm from -3.5 mm for 15° cut-off angle to 5.7 mm for 5° cut-off angle.

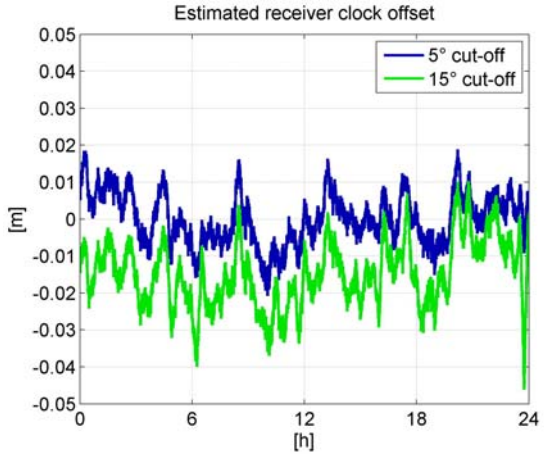

Fig. 2. Estimated clock offsets for different elevation cut-off angles

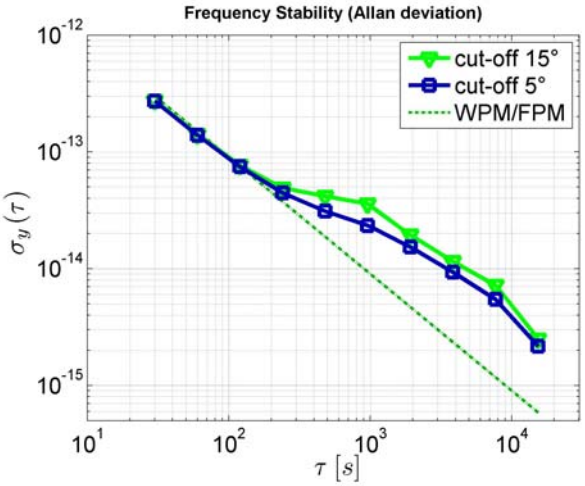

Fig. 3. Allan Deviation of estimated clock offsets

IMPACT OF DIFFERENT MAPPING FUNCTIONS

The mapping functions in use today are almost identical for elevation angles greater than 15°, at lower elevations however they are significantly different. In order to analyze the impact of different mapping functions on the estimated receiver clock, we have tested three frequently used mapping functions (Tab. 2). The coefficients of the Niell Mapping Functions (NMF) [14] have been derived from a fit to radiosonde data across north America. This mapping function has been very popular due to its accurate results and its simple usage. The NMF requires only the day of year, the station height and the station latitude as input parameters to determine the coefficients. Its main disadvantage is the poor performance in southern latitudes, Antarctica in particular. This Problem has been resolved with the newer Global Mapping Functions (GMF) [13] which is based on 3 years of data from a global numerical weather model. The usage of GMF is essentially the same as the Niell mapping functions only the station longitude has to be known in addition. Both NMF and GMF are limited in the fact, that they apply average seasonal coefficients but do not take into account the actual (in situ) atmospheric conditions during the time of the observation. This limitation is overcome with the Vienna mapping functions (VMF1) that are based on ray tracing through multiple pressure levels of a numerical weather model [8]. The coefficients for the computation of the VMF1 are currently provided on a 2°x2.5° grid with 6 hour intervals. The respective files can be downloaded from the VMF web site (http://mars.hg.tuwien.ac.at/~ecmwf1/VMFG/).

Table 2. Troposphere mapping functions analyzed in this study

Model	MF	A priori ZHD
1	NMF	STD
2	GMF	STD
3	VMF1	STD

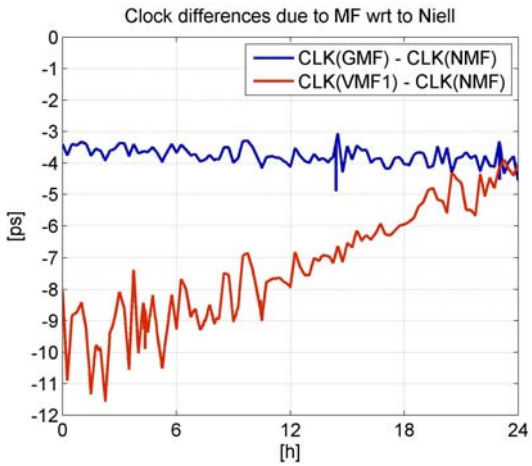

Fig. 4. Receiver clock differences using GMF and VMF1 with respect to NMF (elevation cut-off angle: 5°)

Fig. 4 shows the clock differences when using GMF and VMF1 instead of NMF for our test data. We see that, the differences with respect to the older NMF may exceed 10 ps mainly caused by an offset and drift. Apart from these long-term variations, the differences reach a few ps only. The difference of the station height with respect to the weekly IGS solution is 6.7 mm for the NMF, 5.7 mm for the GMF and 4.9 mm for the VMF1.

IMPACT OF HYDROSTATIC ZENITH DELAY MODELS

Hydrostatic and wet mapping functions differ significantly for elevation angles below 10°. Thus an error in the modeled hydrostatic troposphere delay cannot be fully absorbed by the estimated wet zenith delay. This effect is often called dry-wet separation error. In order to study this effect we have analyzed PPP solutions with different strategies to model the hydrostatic troposphere delay (Tab. 3). The non-hydrostatic zenith delay was estimated as part of the PPP solution with the elevation cut-off angle set to 5°. In a first run we applied a standard atmosphere with a reference pressure of 1013.25 hPa at sea level. This value has been corrected for the station height using the model of Berg [15] and then used to compute the a priori hydrostatic delay according to Saastamoinen [16]. The Saastamoinen model was also used in the second run but the pressure value was taken from the Global Pressure and Temperature (GPT) model by Böhm et al. [17]. In the third run the hydrostatic zenith delay was derived from a numerical weather model, more precisely the European Center for Medium-Range Weather Forecast (ECMWF). These ZHD values are provided with 6 hour resolution on a global 2° by 2.5° grid along with the coefficients of the Vienna Mapping Function I.

Fig. 5 shows the hydrostatic zenith path delays as derived from the three models. For reference the ZHDs derived from observed pressure values at the site have also been plotted. The ZHDs differ by several centimeters. The standard atmosphere and GPT models are constant for an entire day whereas the ECMWF based ZHDs are piece-wise linear with 6 hour intervals. The different ZHDs are largely compensated by the estimated ZWDs (Fig. 6) and to a small degree by the estimated station height. Consequently, the receiver clock estimates for the chosen example differ by an offset of a few millimeters and variations of 1 mm at maximum (Fig. 7). Interestingly, the receiver clock differences do not follow the changes in the ECMWF derived ZHD. Instead the non-constant differences are absorbed into the estimated ZWD (Fig. 6). The difference of the station height with respect to the weekly IGS solution is 5.7 mm for the ZHD derived from the standard atmosphere, 3.9 mm for GPT and 7.6 mm for the ECMWF based ZHD.

Table 3. Comparing the influence of different ZHD models

Model	MF	A priori ZHD
1	GMF	STD
2	GMF	GPT
3	GMF	ECMWF

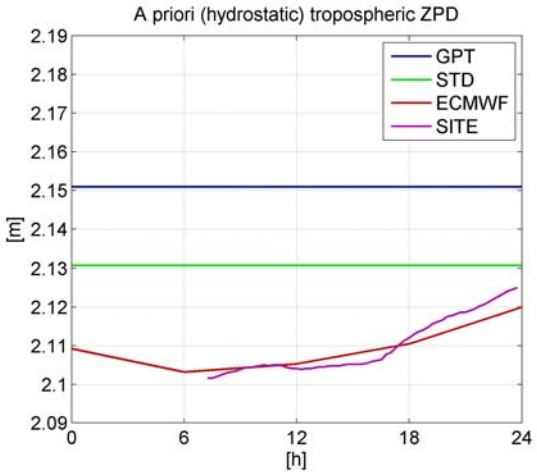

Fig. 5. Different models for the (a priori) hydrostatic zenith delay (ZHD)

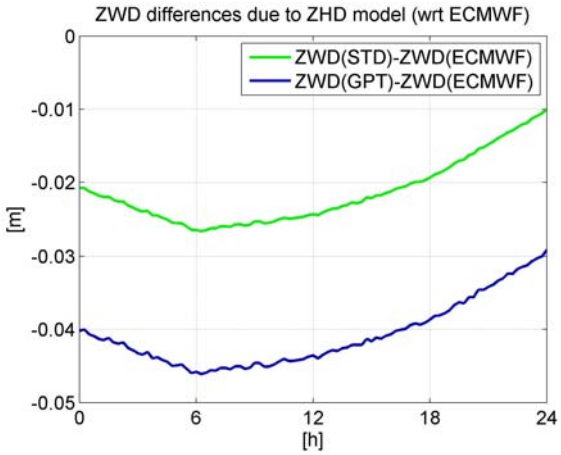

Fig. 6. Difference of the estimated ZWD for different ZHD models wrt to ECMWF based values

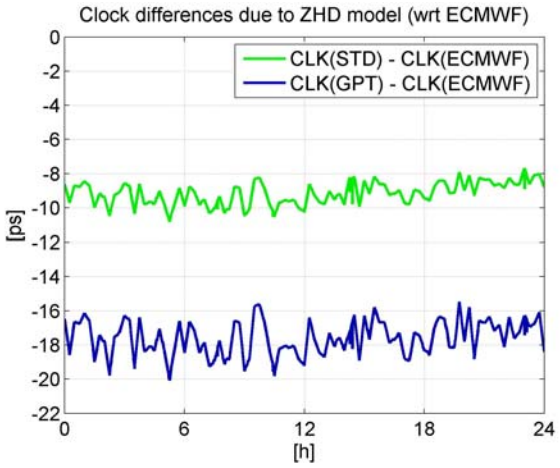

Fig. 7. Differences of the estimated receiver clock when using ZHD values derived from a standard atmosphere and GPT wrt to ECMWF derived values

CONCLUSIONS

We have given a brief overview of the conventional troposphere modeling strategy for GNSS analysis. Subsequently we have shown that a ZWD error is mapped into the estimated receiver clock with a factor of 1.4 to 2.4 depending on the elevation cut-off. Furthermore, we have demonstrated that by including low elevation data into the PPP solution, the peak variations in the receiver clock can be reduced and the ZWD estimates become more stable.

In addition we have analyzed the impact of the hydrostatic zenith path delays and the mapping function for estimating the wet part of the zenith delay. It turned out, that the estimated clock offsets are not very sensitive to the mapping function and the strategy to model the hydrostatic zenith delays. Even the latest mapping functions based on NWM data did not lead to a substantial reduction of the noise level of the clock estimates at sub-daily timescales. This is probably due to the low temporal and spatial resolution and the inherent azimutal symmetry of all the mapping functions failing to model any small-scale tropospheric fluctuations. However, more data needs to be analyzed if we want to specify an upper bound for the errors that can be caused by conventional seasonal mapping function and ZHD models.

REFERENCES

[1] J. Dow, R. Neilan and G. Gendt, "The International GPS Service: celebrating the 10th anniversary and looking to the next decade," *Adv Space Res* 36(3):320–326, 2005.

[2] J. Kouba and P. Héroux, "Precise Point Positioning Using IGS Orbit and Clock Products," *GPS Solutions*, vol. 5, pp. 12-28, 2001.

[3] A. Bauch et al., "Comparison between frequency standards in Europe and the USA at the 10^{-15} uncertainty level," *Metrologia*, vol. 43, pp. 109–120, 2006.

[4] R. Dach, T. Schildknecht, U. Hugentobler, L.G. Bernier, G. Dudle, "Continuous geodetic time-transfer analysis methods", *IEEE transactions on ultrasonics, ferroelectronics and frequency control* 53(7), pp. 1250-1259, July 2006.

[5] U. Weinbach and S. Schön, "Evaluation of the Clock Stability of Geodetic GPS Receivers Connected to an External Oscillator," *Proceedings of the ION GNSS*, Savannah, GA, USA, 2009.

[6] M. Bevis, S. Businger, T. A. Herring, C. Rocken, R. A. Anthes, and R. H. Ware, "GPS Meteorology: Remote Sensing of Atmospheric Water Vapor Using the Global Positioning System," *J. Geophys. Res.*, 97(D14), 15,787–15,801, 1992.

[7] D. McCarthy and G. Petit, "IERS Conventions (2003)," *IERS Tech. Note 32*,Verlag des Bundesamtes für Kartographie und Geodäsie, Frankfurt, Germany, 2004

[8] J. Boehm, B. Werl and H. Schuh, "Troposphere mapping functions for GPS and very long baseline interferometry from European Centre for Medium-Range Weather Forecasts operational analysis data," *J. Geophys. Res.*, 111, B02406, 2006.

[9] P. Bosser, O. Bock, C. Thom, J. Pelon and P. Willis, "A case study of using Raman lidar measurements in high accuracy GPS applications," *Journal of Geodesy*, doi:10.1007/s00190-009-0362-x, 2009

[10] M. Rothacher and G. Beutler, "The role of GPS in the study of global change," Physics and Chemistry of The Earth, Vol. 23, Nr. 9-10, pp 1029-1040, Elsevier Science, 1998.

[11] R. Dach, G. Beutler, U. Hugentobler, et al., “Time transfer using GPS carrier phase: error propagation and results,” *Journal of Geodesy*, vol. 77, no. 1-2, pp. 1–14, 2003.

[12] K. Hackman and J. Levine, “Adding water vapor radiometer data to GPS carrier-phase time transfer,” *Proc. 36th PTTI*, Washington, 2004

[13] J. Böhm, A. E. Niell, P. Tregoning and H. Schuh, “The Global Mapping Function (GMF): A new empirical mapping function based on data from numerical weather model data,” *Geophysical Research Letters* 33, 2006.

[14] A. E. Niell, ”Global mapping functions for the atmosphere delay at radio wavelengths,” *J. Geophys. Res.*, 101, B2, 3227-3246, 1996.

[15] H. Berg, *Allgemeine Meteorologie*. DümmlerVerlag, Bonn, 1948.

[16] J. Saastamoinen, “Contribution to the theory of atmospheric refraction,” *Bulletin Geodesique* 107,13-34, 1973.

[17] J. Böhm, R. Heinkelmann and H. Schuh, “Short note: A global model of pressure and temperature for geodetic applications,” *Journal of Geodesy*, Vol. 81, No. 10, pp. 679-683, 2007.